



A Database-Driven Study on Durability and Sustainability of 3D Concrete Printing Mixtures

Ece Öztürk¹, Yuri Borgianni¹, Ceren Ince²

¹Faculty of Engineering, Free University of Bozen-Bolzano

²Institute for Sustainable Built Environment, School of Energy, Geoscience, Infrastructure and Society, Heriot-Watt University

Abstract

3D concrete printing (3DCP) is gaining attention for its potential in structural and infrastructural applications. While a substantial body of research focuses on developing mixtures for extrusion-based 3DCP, most studies emphasize mechanical performance, while durability and sustainability remain less explored despite their importance for long-term structural reliability and environmental impact. This study addresses this gap through a literature-based comparative database, which compiles mix designs, material replacement types and proportions, and corresponding mechanical and durability parameters. Lower-bound, upper-bound, and favourable performance ranges are identified to allow cross-comparison of mixtures. Results are categorized according to the type of material replacement, namely binder, aggregates, fibres, or additives, and durability-related indicators are evaluated together with sustainability outcomes derived from life cycle assessment. The findings show that moderate binder replacement (15–30%) provides the most balanced performance, maintaining strength and durability while reducing climate change impacts by up to 24%. Aggregate replacement enhances mechanical properties and helps save resources, although its environmental benefits are more limited. Fibre inclusion improves compressive strength and reduces porosity and water absorption, but increases embodied impacts up to 19%, while additives improve fresh-state behaviour only at very low dosages, beyond which porosity, strength losses, and emissions rise sharply. Overall, by jointly considering mechanical performance, durability, and sustainability impacts, this study provides an integrated perspective to support informed mixture optimisation for more durable and environmentally responsible 3DCP applications.

© 2026 The Authors. Published by IEREK Press. This is an open-access article under the CC BY license (<https://creativecommons.org/licenses/by/4.0/>). Peer review under the responsibility of Resourceedings's International Scientific Committee of Reviewers.

Keywords

3D concrete printing; Durability assessment; Life cycle assessment; Material replacement; Literature-based database

1. Introduction

Three-dimensional concrete printing (3DCP) is often presented as a pathway to more efficient and sustainable construction. The technology eliminates formwork, reduces labour, and allows design freedom, all of which suggest significant material and economic savings (Banihashemi et al., 2025). At the material level, printable mixtures differ significantly from conventional cast concretes. Conventional cast concretes rely heavily on coarse aggregate, which makes up the largest share of the mixture and reduces cement demand. In contrast, printable concretes depend on binders and sands to secure pumpability and extrusion stability. The reliance on high cement dosages represents a

critical limitation for 3DCP. Compared to traditional structural concretes, 3DCP mixtures typically rely on higher cement contents (Motalebi et al., 2024). Cement production alone accounts for 8–9% of global CO₂ emissions, while high binder ratios in printable mixtures are associated with increased autogenous shrinkage and vulnerability to aggressive agents due to pore connectivity and interlayer anisotropy (Bentz & Jensen, 2004; Li et al., 2020; Nodehi et al., 2022; Worrell et al., 2001; Zhang et al., 2021).

In this regard, material properties and amounts used for 3DCP can help to improve the durability of 3D printed elements. For example, Zhao et al. reported that 65% pozzolan replacement can result in a decrease of chloride ingress, while Yao et al. reported that additives can improve printability, but high dosages can cause entrapped air, which can affect durability (Yao et al., 2022; Zhao et al., 2023). Similarly, process adjustments, such as minimising interlayer time gaps and ensuring controlled curing, help to improve bond quality and reduce transport pathways (De'M Malan et al., 2021). These findings indicate that adjusting material properties and replacement levels can enhance both printability and durability, while also lowering embodied impacts. A growing body of literature investigates material design for 3D printable concretes. On the other hand, durability and sustainability are often examined in isolation. Consequently, an integrated view linking material replacement strategies to mechanical performance, durability, and environmental impacts is required. This paper aims to bridge this gap by analysing how binder, aggregate, additive, and fibre replacements influence durability, compressive strength, and environmental performance in 3DCP. Through the construction of a comparative database and a life cycle assessment, the study seeks to highlight relationships between durability, mechanical enhancement, and sustainability.

2. Methodology

2.1. Literature search, database construction, and data evaluation

The literature search was carried out in Scopus in August 2023. Combinations of search terms such as “3D print*”, “additive menu*”, “concrete”, and “mortar” were used in the fields “Title”, “Abstract”, and “Keywords”. The search was deliberately broad to capture a wide scope of relevant studies, which initially yielded 2,039 articles. After this stage, articles were removed if they were duplicates, out of scope, lacked extractable mix design information, or focused solely on geopolymer-based systems. The database was constructed by retaining studies that reported clearly defined mix design proportions together with corresponding mechanical and/or durability outcomes, while studies with insufficient methodological detail or outside the scope of extrusion-based 3D concrete printing were not considered further.

Following the screening process, only papers that reported both printed and cast compressive strength results and/or durability parameters were retained, which reduced the dataset to 85 articles. Within this dataset, 14 studies focused on binder replacement, 20 on aggregate replacement, 8 on additive inclusion, and 17 on fibre inclusion, while 26 investigated more than one replacement type. Following the screening process, 85 articles were retained. The full list is not reported here for the sake of brevity. Interested readers can ask for the list of selected articles from the corresponding author. Representative and relevant papers belonging to the database can be found in subsections of Section 3 according to their scope and replacement materials. In terms of materials, silica fume, recycled coarse aggregate, steel fibres, and superplasticizers were the most frequently studied replacements for binders, aggregates, fibres, and additives, respectively. These materials were chosen as the focus for the sustainability assessment.

Then, from the database, we extracted mix design variables, replacement levels, and reported mechanical and durability test results. For compressive strength evaluation, results were considered from casted specimens as well as from printed specimens tested perpendicular to the printing direction, with data obtained from 47 studies. Among the durability properties, porosity and water absorption were the parameters most consistently reported across all replacement types with comparable testing methods and in more than eight studies. Other properties, including freeze–thaw resistance (8 studies), chloride ingress (7 studies), and carbonation (5 studies), were evaluated separately (see Section 3.2.3). Porosity and water absorption were therefore used as primary indicators to support a consistent comparison of transport-related behaviour across the analysed studies. Given the diversity of experimental setups, test protocols, and the low number of studies reported in the literature, durability-related properties such as freeze–thaw resistance, chloride ingress, and carbonation were considered to provide complementary insight into durability

behaviour rather than to serve as directly comparable quantitative metrics. For each assessment, the maximum, minimum, and favourable cases were identified based on the reported performance of the mixtures. Favourable values were identified as replacement levels that consistently maintained or improved mechanical strength while simultaneously exhibiting acceptable durability performance within the reported range. As each performance indicator responds differently to material replacement and the available literature data vary across parameters, slight differences in favourable values may appear. These values are therefore interpreted based on the overall trends in the compiled dataset and should be regarded as approximate ranges rather than exact thresholds. This approach made it possible to highlight not only the extremes of performance but also the practical ranges that appear most suitable for 3D printable concrete.

Different test methods were found in the database, such as X-ray computed tomography (XCT), mercury intrusion porosimetry (MIP), and ASTM-based test methods. Among these, XCT was the most diffused one, with data reported in 19 studies. XCT is a non-destructive imaging technique that provides a three-dimensional visualization of pore networks, enabling quantification of porosity, pore size distribution, pore volume, and internal connectivity. In contrast, MIP allows the detection of smaller pores but reports only pore-throat diameters rather than actual cavity sizes. (Zeng et al., 2020), while ASTM-based water absorption methods measure only water-accessible porosity (Safiuddin & Hearn, 2005). Therefore, only studies using the XCT method were analysed when it comes to porosity evaluation. For the water-absorption test, data are extracted from studies employing comparable immersion–drying methodologies under standardized conditions, with data obtained from 12 studies.

2.2. Sustainability assessment

Subsequently, a cradle-to-gate life cycle assessment (LCA) was performed in accordance with the principles of ISO 14040 and ISO 14044 to quantify the environmental impacts associated with representative replacement materials and replacement ratios in 3D printable concrete. Representative mixtures were defined for each replacement type (binder, aggregate, additive, and fibre), based on typical mix proportions and replacement ranges identified in our database and in the literature at large, e.g., (Hack et al., 2022). For the scopes of the LCA, the functional unit was defined as the production of 1 m³ of concrete. The transportation distance was assumed to be 30 kilometres for all mixtures. Assessments were made using openLCA 2.5, supported by MS Excel for calculations. The life cycle inventory was sourced from the Evah OzLCI2019 database, and the impact assessment method applied was ReCiPe Midpoint (H) by ecoinvent v3.11 LCIA Methods. The results related to climate change, ozone depletion, and freshwater eutrophication are reported in this paper.

Following the LCA, a comparative analysis of each replacement type was carried out using radar charts to visualize their performances. In this stage, the maximum, minimum, and favourable replacement levels identified in Section 2.1 were used as reference points. Each replacement type was evaluated simultaneously across the selected mechanical and durability indicators, as well as its associated emissions calculated through the LCA. In cases where experimental data were not available for a specific replacement amount, corresponding values were estimated from the fitted trendlines derived from the database. This comparison makes it possible to evaluate the interactions between mechanical performance, durability properties, and sustainability. The fitted trendlines were derived from experimentally reported data across different material systems and replacement ranges and were used to compare different replacement types. Given the heterogeneous nature of literature data, these values are intended to reflect a general behaviour rather than the exact material effects. Consequently, the trendlines serve to support the analysis of relative interactions between performance indicators while acknowledging an inherent level of uncertainty. Across the compiled dataset, dispersion is visible in the figures, reflecting the variability reported in the literature, since the data originates from independent studies employing different mix designs, material systems, and experimental conditions. As an indication of this variability, the standard deviation across the dataset is 12.5 for porosity, 7.2 for water absorption, and 0.22 for the printed-to-cast compressive strength ratio. These values mainly reflect differences in materials, methodologies, and testing conditions across the literature sources.

3. Results

3.1. Durability

In this section, the durability properties of 3D printed concretes are evaluated. The focus is on the key mechanisms that determine long-term performance, including freeze–thaw resistance, chloride penetration, and carbonation, which are reported most diffusely in the literature.

3.1.1. Freeze and thaw, chloride penetration, and sulphate attack tests

Freeze–thaw resistance, chloride ingress, and carbonation play a critical role in the long-term performance of 3D printed concrete. Previous studies highlight that weak interlayer regions and entrapped porosity inherent to extrusion make printed elements particularly vulnerable to frost damage (Assaad et al., 2020). Nonetheless, material selection and targeted replacements can mitigate such effects. For example, Zhang et al. (2021). reported that mixtures with higher sand-to-binder ratios performed best, followed closely by those containing polypropylene fibres. In another investigation, concretes produced with alternative binders exhibited lower mass loss than those based on white cement. (Özalp & Dilşad Yilmaz, 2020). Skibicki et al. (2022) confirmed that durability depends strongly on replacement level: recycled PET aggregates at high contents (30–50%) significantly reduced frost resistance, causing strength losses up to 80% after cycling, whereas low PET contents ($\leq 10\%$) preserved satisfactory resistance. Polymer modification has also proven beneficial; Assaad et al. found that styrene–butadiene rubber (SBR) enhanced the flexibility of interfacial zones and was more effective than air entrainment in limiting freeze–thaw deterioration. (Assaad et al., 2020).

Chloride ingress presents another major durability challenge. Van der Putten et al. demonstrated that prolonged time gaps between successive layers markedly increased chloride penetration due to the formation of interfacial microcracks and higher porosity. (Van Der Putten et al., 2022). Malan et al. further showed that elongated and interconnected pores in the interfacial regions created defects such as torn layers, with printed specimens displaying higher chloride conductivity and lower durability indices than cast concrete. (De’M Malan et al., 2021). On the material side, however, certain replacements improve performance. Incorporating supplementary cementitious materials such as GGBS and clay brick powder decreased chloride migration by refining pore structure and enhancing chloride binding capacity. (Zhao et al., 2023). Conversely, untreated recycled aggregates increased chloride ingress due to their higher porosity, while CO₂-pretreated recycled fine aggregates helped mitigate this effect. In addition, Yuan et al. also reported that polyacrylamide addition improved interlayer bonding and indirectly reduced chloride transport. (Yuan et al., 2022).

Carbonation resistance exhibits a similarly complex relationship with material selection. Malan et al. reported that 3D printed specimens generally exhibited higher carbonation depths than cast concrete, owing to elongated pores at interlayer regions. (De’M Malan et al., 2021). Nevertheless, alternative approaches led to limited carbonation in printed concretes. Accelerated CO₂ curing of mortars increased early-age strength, densified the microstructure, and sequestered significant CO₂, thereby lowering long-term carbonation rates. (Wang et al., 2023). Likewise, the use of carbonated bottom slag granules as aggregates reduced carbonation depth by both refining the pore network and storing CO₂ (Butkute et al., 2023). Binder chemistry turned out to be critical too: mixtures with a higher content of medium-heat Portland cement had a 52.4% lower carbonation depth at 28 days compared with those dominated by high-belite sulfoaluminate cement, confirming that carbonation resistance can be tuned through binder selection. (Wang et al., 2021).

These results show that freeze–thaw resistance, chloride ingress, and carbonation are closely linked to pore structure and interlayer quality. Porosity and water absorption serve as key indicators of how readily water and aggressive agents can penetrate the printed matrix. Özalp & Dilşad Yilmaz (2020) showed that lower capillary water absorption reflected a denser microstructure, which also corresponded with reduced mass loss after freeze–thaw cycling and lower chloride permeability. Similarly, Wang, L. et al. (2022) found that increased porosity in interfacial regions of 3D-printed specimens was linked to greater mass loss and reduced frost resistance. These findings show that durability is influenced by pore structure and transport properties, with material selection and replacement level being key

factors. The following section, therefore, examines porosity and water absorption in detail, together with examining different material replacement types.

3.2. Pore structure and transport properties

3.2.1. Porosity

Figure 1 presents the relationship between porosity and material replacement ratios, considering only data obtained with XCT. It was observed that the data is denser for replacement ratios ranging from 3 to 10%.

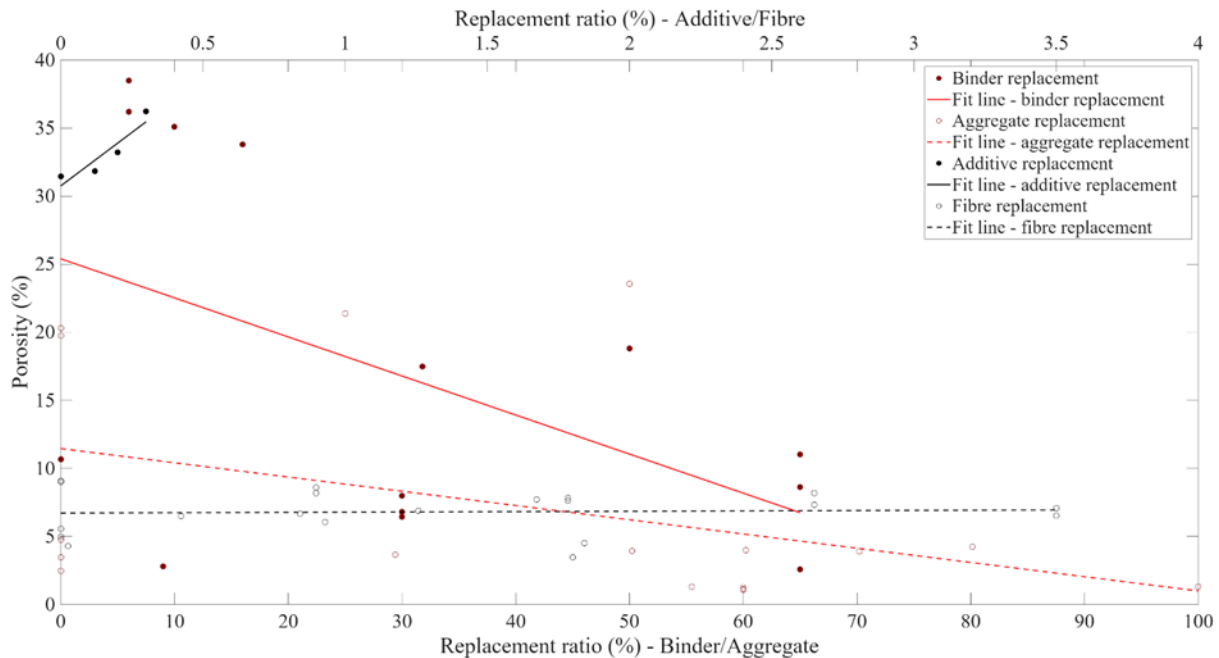


Figure 1. Effect of binder, aggregate, additive, and fibre replacement ratios on porosity(prepared by the authors)

In general, binder-replaced mixes exhibit higher porosity values at lower replacement ratios. Most of the binder replacement data comes from studies using pozzolanic or pozzolanic-potential materials such as fly ash, silica fume, GGBS, and other waste-derived binders with maximum reported replacement levels of 65%. These materials can refine the pore structure through secondary hydration products and improved particle packing, while also influencing rheology by moderating cement hydration rates. (Duan et al., 2022; Zhao et al., 2023). Zhao et al. observed that replacing OPC with 65% GGBS reduced porosity by approximately 20%, whereas a 30% GGBS replacement resulted in a slight (~4%) increase. (Zhao et al., 2023). Liu et al. reported that replacing 16% silica fume for OPC led to a ~7% reduction in porosity. (Liu, C. et al., 2023b). Such trends suggest that the relationship between replacement ratio and porosity is non-linear, with lower replacement levels often linked to higher porosity values—likely due to insufficient filler effect and incomplete pozzolanic reactions. Higher replacement ratios appear to benefit from denser packing and more extensive secondary C–S–H formation. (Slavcheva, 2019). Based on these findings, 30% binder replacement is identified as the optimal level to maximise porosity reduction.

Aggregate replacement was generally associated with lower porosity values than binder replacement. In many studies, porosity decreased as the replacement ratio increased, although some variations were observed depending on the type and characteristics of the aggregates used. Most of the reported data is related to coarser aggregate replacement. Some studies observed that increasing coarse aggregate content leads to higher porosity. (Hao et al., 2022; Wang, X. et al., 2022), while others reported the opposite effect (Deng et al., 2022; Liu, H. et al., 2022b). Hao et al. showed that an increase in recycled coarse aggregate (50%) increased porosity of approximately 20% (Hao et al., 2022). Instead, Deng et al. (2022) reported that clay ceramsite coarse sand replacement could yield significantly lower porosity (up to 3 times) than the control condition. (Deng et al., 2022). Only one study examined the influence of desert sand content, reporting that increasing the sand: binder ratio could reduce porosity up to 16% due to the fine grading of desert sand filling micro voids within the matrix. (Wang, L. et al., 2022). Therefore, a favourable value for aggregate replacement is 60% by, considering the low porosity values in Figure 1.

Additive replacement, which involves HPMC and foaming agents, leads to an increase in porosity to an extent larger than other replacement types. Markedly, the higher the additive replacement ratio, the higher the exhibited porosity values. Although only one study reported porosity values measured via XCT for additive inclusion, other studies have also indicated that rheology modifiers can increase porosity. This effect is primarily linked to their tendency to delay cement hydration, increase the amount of entrapped air, and consequently increase interlayer porosity. (Hack et al., 2022). For instance, Pasupathy et al. (2022) observed that the use of a foaming agent could increase porosity by up to 40% due to bubble coalescence and merging, while Liu, C. et al. (2023b) found that HPMC addition led to the formation of larger pores. Considering the dataset in Figure 1, an inclusion level of 0.12% additive content appears to be the most favourable, as it resulted in the smallest increase in porosity among the tested dosages.

Fibre replacement mostly yielded low and consistent porosity values across the dataset. The studies investigating the effects of fibre inclusion are mostly about carbon and steel reinforced mixtures. Rutzen et al., and Liu, J. et al.(2023) reported that high fibre content may counteract compaction of the matrix, which may be caused by the air entrapped during the mixing process. On the other hand, Pham et al. (2020) reported that the increase in steel fibre resulted in a decrease in porosity by up to around 35%, which can be attributed to the potential of bridging microcracks during printing and enhancing structural integrity between layers. Therefore, the identified optimum value for fibre replacement is 1.8% due to the concentration of low porosity values in this area of Figure 1.

3.2.2. Water absorption

Water absorption results across different replacement values are illustrated in Figure 2. Accumulation of data is observed in the range of 8-13% of the replacement ratio.

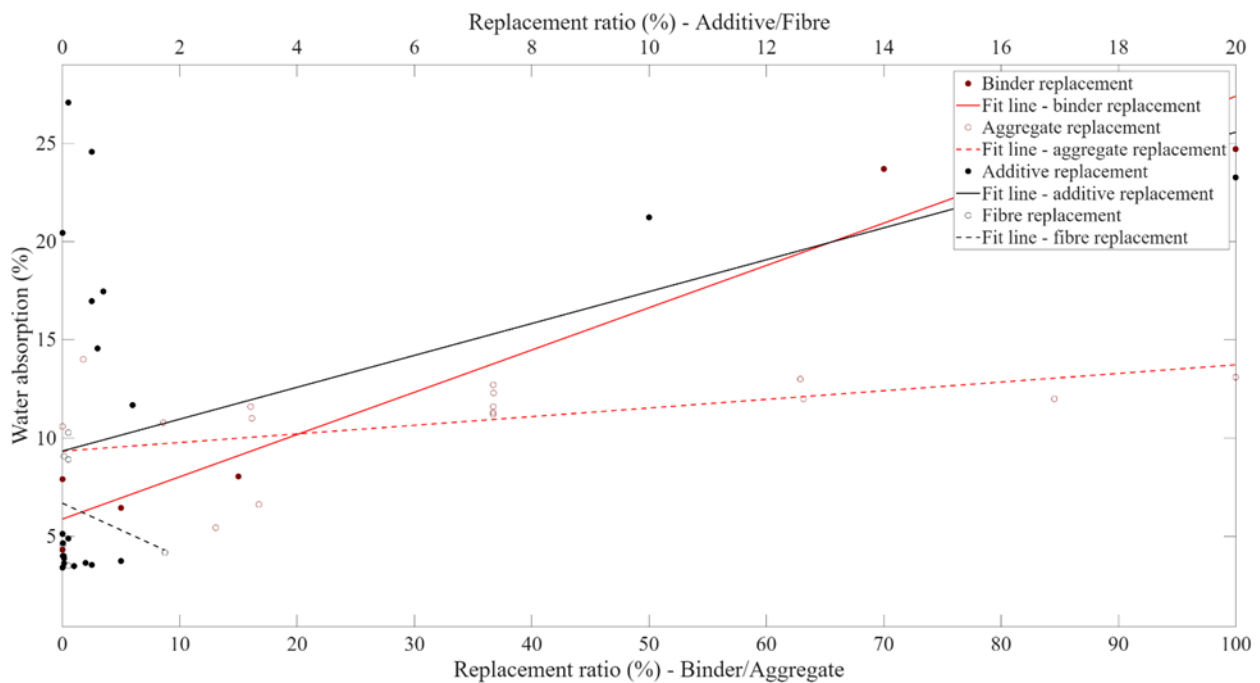


Figure 2. Water absorption behaviour of 3D printable concretes depending on binder, aggregate, additive, and fibre replacement ratios(prepared by the authors)

In the case of binder replacements, most studies investigated pozzolanic materials across a replacement range of 0–100%. The dataset shows a general tendency for water absorption to increase with higher replacement levels. For example, Barbosa et al. (2022) reported that 15% metakaolin replacement almost doubled the water absorption relative to the reference mixture. In contrast, Jaji et al. (2024) observed that replacing 5% slag with metakaolin decreased absorption by approximately 20%. Similarly, Butkute et al. (2023) found that a mixture containing 70% bottom slag ash and burnt shale had around 10% lower water absorption than one with 92% replacement. These variations can be attributed to the effect of high replacement levels on the pore structure: excessive binder replacement reduces matrix densification and generates additional capillary voids, thereby facilitating water ingress. From the

available data, a binder replacement level of 15% appears to be the most favourable, since absorption values are consistently lower in this range.

Aggregate replacement generally resulted in lower water absorption than binder replacement. Across the reported replacement levels of 0–100%, a slight upward trend in absorption was observed. The majority of the available data relate to filler-type aggregates. For instance, Barbosa et al. and Araújo et al. reported that increasing the proportion of limestone powder and lightweight expanded clay aggregate led to higher absorption values. This behaviour is consistent with the inherent porosity of these fillers, which contributes to additional capillary pathways in the hardened matrix (Ahmida et al., 2023). An aggregate replacement level of 17% can be identified as favourable, as the lowest absorption values are concentrated around this value.

For additives, the effect on water absorption varied depending on material type. Calcium carbonate, superplasticizers, foaming agents, nanosilica, and nano-TiO₂ were most frequently reported, with replacement levels ranging from 0 to 20%. In general, additions above 10% tend to correspond to lime- or pozzolan-based materials, whereas plasticizers and viscosity-modifying agents are typically incorporated at dosages below 2%. Increases in absorption were generally observed with higher dosages. Calcium carbonate was associated with the most pronounced rise. Vergara & Colorado reported nearly 30% higher absorption, explained by its porous morphology (Vergara & Colorado, 2020). By contrast, Liu, Q. et al. found that nano-TiO₂ reduced water absorption by approximately 30%, a result attributed to densification of the matrix and refinement of pore structure, as confirmed by microscopy (Liu, Q. et al., 2022). Taken together, these results indicate that an additive content of around 1.2% represents a favourable value, since lower absorption results consistently emerge from this dosage onwards.

Fibre inclusion produced a consistent decreasing trend in water absorption across the examined range of 0–2%. The majority of the dataset concerns polypropylene fibres, with one study on basalt fibres. Most of the studies indicated that increasing fibre content reduced absorption with high crack resistance. For instance, Liu, Q. et al. (2022) reported a 6% reduction in absorption with fibre inclusion. On this basis, a fibre content of 0.1% may be regarded as favourable, as the lowest absorption values are clustered in this range.

3.3. Compressive strength ratio

The relationship between replacement ratio and printed-to-casted compressive strength results is presented in Figure 3. Although there is much data dispersion across all replacement types, the normalized compressive strength remains largely between 0.6 and 1.0.

Binder replacement in the reviewed studies is primarily aimed at improving fresh-state properties, such as workability and extrusion stability, and at adjusting setting behaviour for 3D printing applications. All cases in this dataset involve pozzolanic materials, which are the most frequently used binder replacement, with replacement levels ranging from 0–65% and showing a slightly decreasing trend in compressive strength at higher ratios. This reduction is linked to the lower cement content and the slower pozzolanic reaction rate of the replacement materials, which can leave unreacted particles and increase capillary porosity in the early curing stages (Nedunuri et al., 2020). For example, Zhao et al. reported a marked drop in compressive strength when 65% of OPC was replaced with a combination of GGBS and clay brick powder, whereas Vishruthi et al. found that 25% binder replacement using fly ash, silica fume, and GGBS could yield up to six times higher strength compared to the reference mix (Vishruthi et al., 2021; Zhao et al., 2023). Based on these results, a 30% replacement level is identified as favourable, offering a balance between mechanical performance and the benefits of material replacement.

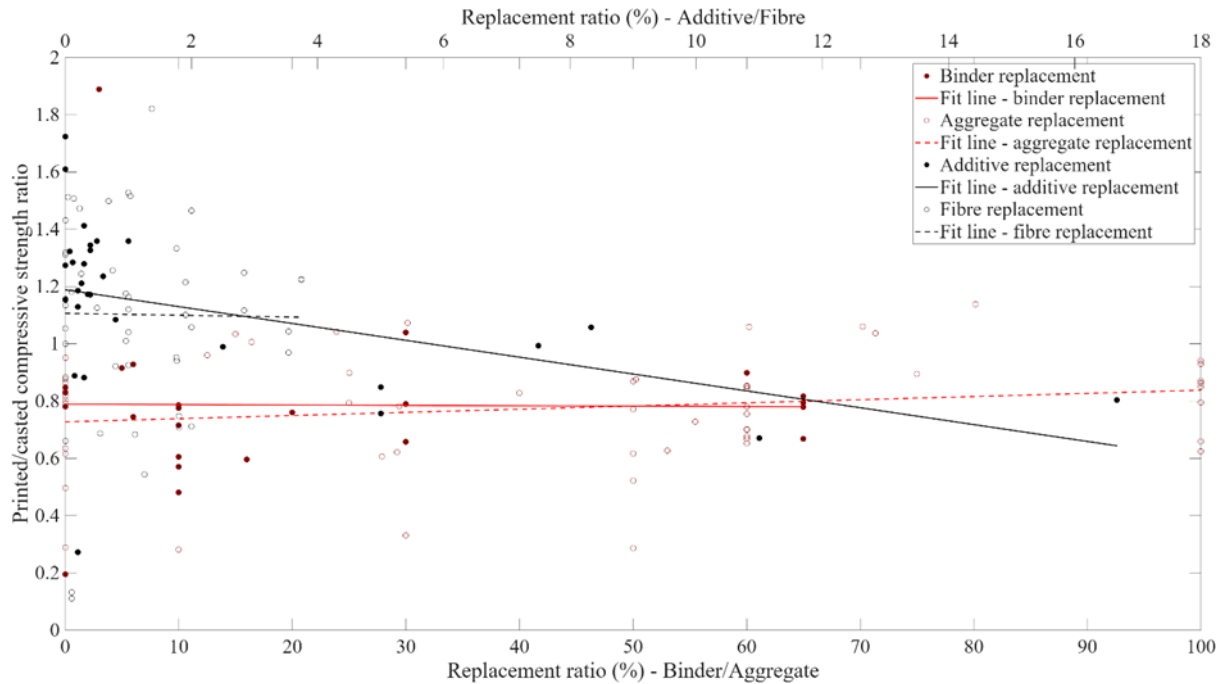


Figure 3. Relationship between material replacement ratio and printed-to-cast compressive strength ratio (prepared by the authors)

The aggregate replacement group covers a range of 0–100%, including recycled coarse and fine aggregates, waste materials, fillers, and other alternatives. Most of the studies focus on the inclusion of coarser aggregates. Overall, most studies show an increasing trend in compressive strength with higher aggregate replacement. This improvement is often linked to better particle packing, enhanced interfacial transition zones (ITZ), and in some cases, reduced matrix porosity. For example, Liu, H. et al. (2022a) reported that using 60% natural coarse aggregate increased compressive strength by 15% due to improved particle interlocking and load transfer. (Deng et al., 2022) found that pre-wetted lightweight aggregates lowered porosity, leading to higher specific strength at moderate replacement ratios (Deng et al., 2022). Coated recycled crumb rubber also improved particle bonding, slightly offsetting the losses normally seen with rubber inclusion. (Liu, J. et al., 2022). However, some cases showed strength reductions. Liu, C. et al. (2023a) observed that higher recycled sand content gave rise to numerous loose pores, reducing matrix compactness. Bai et al. (2023) reported that 100% quartz sand replacement lowered strength by 7.2%, to be attributed to weaker particle–paste bonding, poorer packing, and a more porous ITZ. In consideration of this data, a 60% replacement level is identified as favourable for aggregate replacement in 3DPC.

As far as additive replacement is concerned, this dataset primarily includes nanosilica, phase-changing materials, superplasticizers, hydroxypropyl methylcellulose (HPMC), and foaming agents. Most studies reported that increasing the content of rheology-modifying additives, such as HPMC or foaming agents, led to a reduction in compressive strength, mainly due to increased entrapped air and larger pore formation, which weakens the matrix. (Hack et al., 2022; Liu, C. et al., 2023b; Markin et al., 2021). For instance, the inclusion of foaming agents was found to reduce compressive strength, which is attributed to lower density and higher porosity. (Pasupathy et al., 2022). In addition, Cui et al. (2022) also reported that 20% phase changing material (PCM) inclusion resulted in 37.5% decrease in compressive strength due to the weak bonding between PCM and cement particles. Based on the data reported in Figure 3, an additive content of around 0.3% is identified as favourable.

The fibre inclusion group covers replacement levels between 0–3.75%, with studies focusing on steel, polypropylene (PP), polyethylene (PE), polyvinyl alcohol (PVA), basalt, glass, and carbon fibres. Most of the studies focus on steel fibres. Overall, fibre addition generally improves compressive strength, while higher amounts may cause a reduction in some cases. This behaviour is linked to fibre–matrix interaction and pore structure changes (Yang et al., 2022). Fibres can enhance crack-bridging capacity, delay crack propagation, and provide better mechanical properties (Liu, J. et al., 2023; Tan et al., 2025). For example, Singh et al. (2022) reported that adding 0.75% steel fibres increased compressive strength by 3%, attributed to improved stress transfer and reduced microcracking. Similarly, Liu, J. et

al. (2023) found that milled recycled carbon fibres increased strength due to a refined pore structure and improved bonding. In contrast, high fibre contents can lead to fibre agglomeration, poor dispersion, and entrapped air, which weaken the matrix and reduce strength (Jiang et al., 2022; Ma et al., 2022). Jiang et al. (2022) observed that PP fibre inclusion reduced compressive strength by 7%, primarily due to increased porosity and weaker fibre–matrix bonding during the printing process. Considering this trend, an optimum fibre content of around 2% appears favourable, balancing mechanical enhancement with minimal negative effects on the matrix.

3.4. Sustainability

Figure 4 presents the results of the environmental assessment across three midpoint impact categories: climate change, ozone depletion, and freshwater eutrophication.

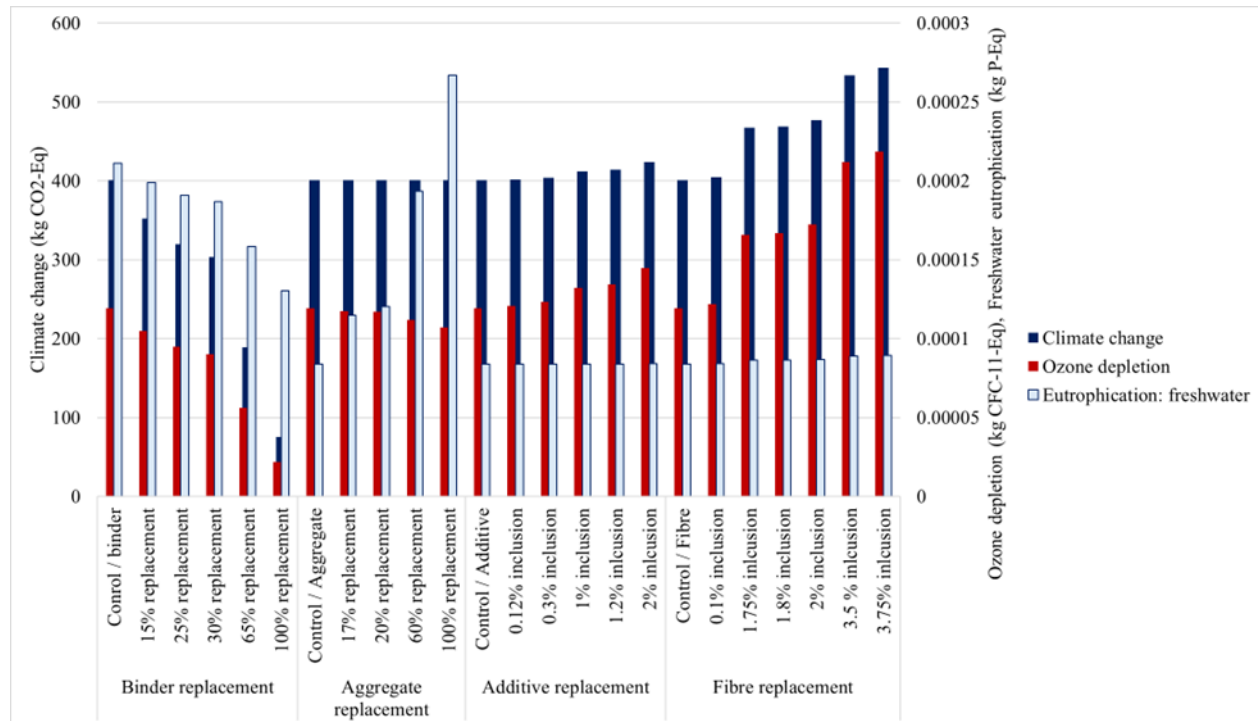


Figure 4. Environmental impacts of material replacements in 3D printable concretes across three categories: climate change, ozone depletion, and freshwater eutrophication(prepared by the authors)

Among all categories, binder replacement emerges as the most effective strategy for reducing environmental impacts. As the level of replacement increases, emissions decline sharply, reflecting the fact that cement is the most carbon-intensive component of the mixture. At 100% binder replacement, the climate change impact is nearly 24% lower than the control mix, with similar reductions observed for ozone depletion and eutrophication. Aggregate replacement, in contrast, leads to only minor changes: a slight increase in climate change impact (around 0.03%), a significant rise in freshwater eutrophication (almost 87%), and a 6% reduction in ozone depletion. The increase in certain categories can be attributed to the additional processing and treatment required when recycling demolition wastes. Nonetheless, aggregate replacement remains important from a sustainability perspective, given that aggregates constitute the largest volume fraction of concrete and their replacement helps conserve natural resources while promoting the reuse of waste materials. By comparison, additives and fibres show a consistent increasing trend across all three categories. Even at low inclusion levels, their high unit impacts result in great environmental burdens, underlining the trade-off between enhanced material performance and sustainability. This highlights an important trade-off. While additives are essential for fresh-state properties and printability, and fibres often deliver the best performance in terms of strength and durability, both contribute to a higher environmental burden. Overall, the figure emphasizes the need to balance mechanical performance, durability, and sustainability by carefully considering not only the type of material used but also the level of inclusion.

3.5. Discussion of results

The radar plots in Figure 5 illustrate the comparative performance of different material replacement strategies in terms of strength ratio, durability indicators (porosity and water absorption), and sustainability categories (climate change, ozone depletion, freshwater eutrophication). The mechanical and durability indicators are derived from the compiled literature database (47 studies for compressive strength, 19 studies for porosity, and 12 studies for water absorption), whereas the environmental indicators are calculated through the LCA model based on representative mixtures defined from the database and optimized replacement levels. Trend-based estimations are used to support the interpretation of overall relationships and trade-offs between mechanical performance, durability behaviour, and environmental impacts across the examined replacement strategies.

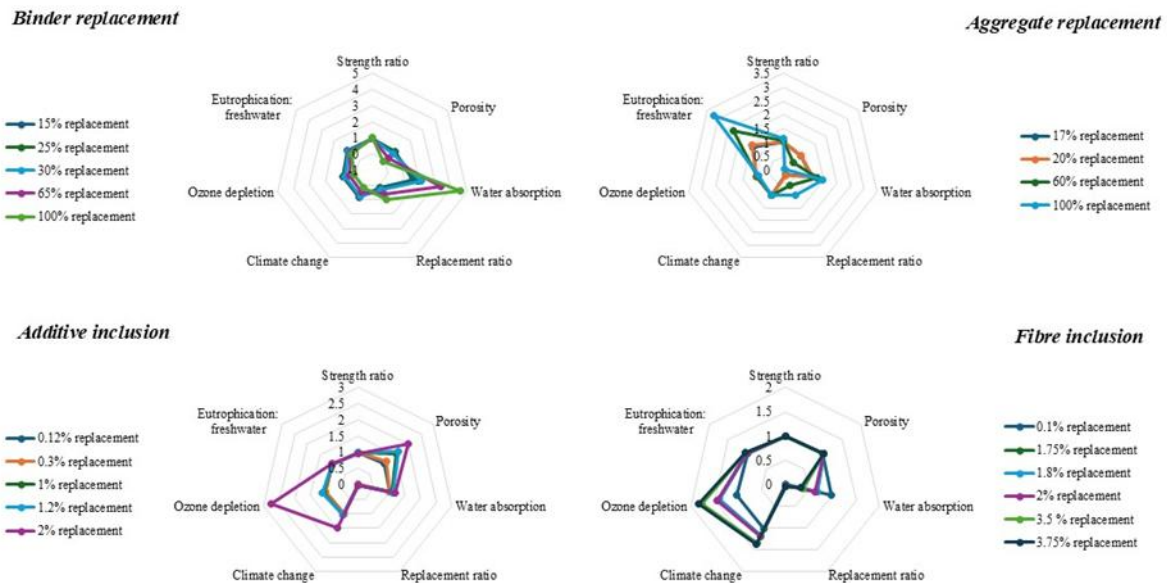


Figure 5. Radar chart comparison of binder, aggregate, additive, and fibre replacements for compressive strength ratio, durability, and sustainability parameters(prepared by the authors)

As illustrated in the figure, binder replacement demonstrates the highest potential for reducing environmental impacts compared to other replacement types. This can be attributed to the fact that cement, among the mixture constituents, is the most emission-intensive material. The replacement level of 100% shows the potential to reduce climate change impacts by nearly fivefold. However, it also results in the highest water absorption values among all replacement strategies. On the other hand, moderate replacement levels of 15–30% provide a more favourable balance. While keeping porosity, water absorption, and compressive strength within an acceptable range, they also offer notable environmental benefits. Specifically, CO₂ emissions can be reduced by approximately 12–25%, ozone depletion by similar extents, and freshwater eutrophication by 5–11%.

For aggregate replacement, increasing the proportion of recycled aggregate does not lead to a substantial reduction in climate change impacts. However, as illustrated in the figure, freshwater eutrophication more than tripled compared to the control mixture. Replacement levels in the range of 17–60%, which are more favourable in terms of porosity, water absorption, and compressive strength, simultaneously reduce freshwater eutrophication by 40–100% and decrease ozone depletion by approximately one-fifth. Beyond the numerical impacts, it is also important to emphasize that increasing the use of recycled aggregate helps save natural resources and contributes to reducing certain environmental burdens. In the case of additives, even small inclusion levels influence porosity, water absorption, and compressive strength, while also causing a substantial increase in environmental impacts. For instance, a 2% inclusion leads to an approximately 30% increase in climate change impacts. By contrast, lower dosages such as 0.12% and 0.3%, which also provide favourable values for porosity, water absorption, and compressive strength, result in much smaller increases: around 0.3–0.9% for climate change, and about 0.012–0.03% for ozone depletion and freshwater eutrophication. Since certain additive levels are necessary to ensure printability, keeping their proportions within this

lower range is key to safeguarding sustainability while meeting performance requirements. As for fibres, similarly to additives, even small replacement ratios can lead to noticeable increases in environmental impacts. Nevertheless, when examining porosity, water absorption, and compressive strength, fibre inclusion often yields some of the most favourable results among the studied strategies. At the highest replacement ratio, climate change impacts increase by approximately 35%. However, for the more favourable range of 0.1–2% inclusion, this increase is limited to 1–19%. In terms of other indicators, ozone depletion rises by 2–22%, while freshwater eutrophication increases by 0.2–2%. These findings suggest that carefully controlled fibre dosages can enhance mechanical performance while keeping environmental burdens at a comparatively moderate level. The environmental results presented in this study are inherently influenced by the underlying assumptions adopted in the LCA, including the definition of the functional unit, the assumed transport distance, the selected impact categories, and the choice of background database. While these assumptions affect the absolute magnitude of the reported impacts, the relative comparison between material replacement strategies is expected to remain robust, as all scenarios were evaluated consistently within the same system boundaries. Accordingly, the results are interpreted as indicative of comparative environmental trends rather than as absolute impact values for specific production contexts.

The results highlight that both durability and sustainability depend strongly on the material selected and the level of its replacement. Small changes in the replacement ratio can shift pore characteristics in opposite directions, either refining the microstructure or amplifying weaknesses that accelerate degradation. At the same time, different replacement strategies have distinct environmental consequences. Reducing cement content can lower emissions significantly, while fibres and additives often increase them despite their mechanical benefits. The synthesis of literature data naturally reflects variations in mix designs, experimental conditions, and reporting approaches across studies. The paper suffers from this heterogeneity because available data prevent scholars from predicting mechanical and environmental performances based on additives and replacements. As such, a current limitation of the paper is the impossibility of optimizing mixes based on specific industrial requirements. On the other hand, the same heterogeneity of conditions in previous literature works enables a broader perspective on material behaviour and overall performance trends in 3D concrete printing, supporting comparative interpretation rather than case-specific conclusions. In this context, the quantitative ranges and favourable replacement levels discussed in this study are best interpreted as indicative trends emerging from the literature, rather than as universally applicable design values.

4. Conclusion

This study shows that the durability and sustainability of 3D printable concretes are closely governed by both the type and the level of material replacement. Binder replacement proved most effective, with moderate levels of 15–30% replacements reducing porosity and water absorption while maintaining compressive strength. Although higher levels (above 65%) led to mechanical losses, they also delivered the greatest environmental benefits, lowering climate change impacts by nearly 24%. Aggregate replacement results between 17% and 60% improved pore structure and compressive strength, yet their environmental impact was less consistent, with only marginal reductions in climate change potential and notable increases in freshwater eutrophication linked to recycled aggregate processing. Additives were found to have a strong dosage-dependent effect. At low levels (0.12–0.3%), they maintained acceptable durability and compressive strength with negligible emissions, but higher dosages increased porosity, reduced strength, and raised climate change impacts by up to 30%. Fibre inclusion also enhanced durability and strength at low to moderate levels (0.1–2%), lowering porosity and water absorption, though this came with environmental burdens of 1–19%. When used in excess, fibres caused agglomeration and pore growth, leading to both mechanical and environmental drawbacks.

It should be noted that the favourable replacement levels identified in this study are derived from a comparative analysis of literature data and should therefore be interpreted as indicative trends rather than definitive mix design values. Given the variability in materials, mixture compositions, and testing protocols across the analysed studies, the reported ranges are intended to support a comparative understanding of performance–sustainability relationships in 3D concrete printing rather than to serve as direct design guidelines.

Overall, the results highlight that binder replacement remains the most beneficial strategy for reducing emissions; aggregate replacement contributes mainly to mechanical performance and resource conservation; both additives and

fibres improve structural and durability characteristics but lead to negative environmental consequences. These findings underscore the importance of establishing targeted replacement levels to achieve a balance between mechanical reliability, long-term durability, and sustainability in 3D concrete printing.

Acknowledgment

The abstract of this paper was presented at the 10th Edition Urban Planning & Architectural Design for Sustainable Development (UPADSD) Conference, held from 21 to 23 October 2025.

Funding

This research did not receive any specific grant from funding agencies in the public, commercial, or not-for-profit sector/ individuals

Ethics approval

Not applicable.

Conflict of interest

The author(s) declare(s) that there is no competing interest.

References

- Ahmida, F., Sayah, G. M., Zineb, D., & Quéneudec-t'Kint, M. (2023). Experimental study on the effect of lime and aluminium content on porosity, introduced porosity, compressive strength, and thermal conductivity of a lightweight cellular concrete based on limestone sand. *Construction and Building Materials*, 392, 131552. <https://doi.org/10.1016/J.CONBUILDMAT.2023.131552>
- Araújo, R. A., Martinelli, A. E., Cabral, K. C., F. O. A. Dantas, A., F. D. Silva, I., A. C. Xavier, A., & Santos, A. L. (2022). Thermal performance of cement-leca composites for 3D printing. *Construction and Building Materials*, 349, 128771. <https://doi.org/10.1016/J.CONBUILDMAT.2022.128771>
- Assaad, J. J., Hamzeh, F., & Hamad, B. (2020). Qualitative assessment of interfacial bonding in 3D printing concrete exposed to frost attack. *Case Studies in Construction Materials*, 13, e00357. <https://doi.org/10.1016/J.CSCM.2020.E00357>
- Bai, M., Wu, Y., Xiao, J., Ding, T., & Yu, K. (2023). Workability and hardened properties of 3D printed engineered cementitious composites incorporating recycled sand and PE fibers. *Journal of Building Engineering*, 71, 106477. <https://doi.org/10.1016/J.JOBE.2023.106477>
- Banihashemi, S., Akbarnezhad, A., Sheikhhoshkar, M., Bril El Haouzi, H., & Rolfé, B. (2025). 3D printing in construction: sustainable technology for the building industry. *Progress in Additive Manufacturing*, 1–34. <https://doi.org/10.1007/S40964-025-01314-Y>
- Barbosa, M. S., dos Anjos, M. A. S., Cabral, K. C., & Dias, L. S. (2022). Development of composites for 3D printing with reduced cement consumption. *Construction and Building Materials*, 341, 127775. <https://doi.org/10.1016/J.CONBUILDMAT.2022.127775>
- Bentz, D. P., & Jensen, O. M. (2004). Mitigation strategies for autogenous shrinkage cracking. *Cement and Concrete Composites*, 26(6), 677–685. [https://doi.org/10.1016/S0958-9465\(03\)00045-3](https://doi.org/10.1016/S0958-9465(03)00045-3)
- Butkute, K., Vaitkevicius, V., Sinka, M., Augonis, A., & Korjakins, A. (2023). Influence of Carbonated Bottom Slag Granules in 3D Concrete Printing. *Materials* 2023, Vol. 16, Page 4045, 16(11), 4045. <https://doi.org/10.3390/MA16114045>
- Cui, H., Yu, S., Cao, X., & Yang, H. (2022). Evaluation of Printability and Thermal Properties of 3D Printed Concrete Mixed with Phase Change Materials. *Energies* 2022, Vol. 15, Page 1978, 15(6), 1978. <https://doi.org/10.3390/EN15061978>
- De'M Malan, J., van Rooyen, A. S., & van Zijl, G. P. A. G. (2021). Chloride-Induced Corrosion and Carbonation in 3D Printed Concrete. *Infrastructures* 2022, Vol. 7, Page 1, 7(1), 1. <https://doi.org/10.3390/INFRASTRUCTURES7010001>
- Deng, Z., Jia, Z., Zhang, C., Wang, Z., Jia, L., Ma, L., Wang, X., & Zhang, Y. (2022). 3D printing lightweight aggregate concrete prepared with the shell-packing-aggregate method - Printability, mechanical properties, and pore structure. *Journal of Building Engineering*, 62, 105404. <https://doi.org/10.1016/J.JOBE.2022.105404>
- Duan, Z., Li, L., Yao, Q., Zou, S., Singh, A., & Yang, H. (2022). Effect of metakaolin on the fresh and hardened properties of 3D printed cementitious composite. *Construction and Building Materials*, 350, 128808. <https://doi.org/10.1016/J.CONBUILDMAT.2022.128808>
- Hack, N., Naboni, R., Goulas, C., Laghi, V., Ferretti, E., & Glar Yalçinkaya, Ç. (2022). Influence of Hydroxypropyl Methylcellulose Dosage on the Mechanical Properties of 3D Printable Mortars with and without Fiber Reinforcement. *Buildings* 2022, Vol. 12, Page 360, 12(3), 360. <https://doi.org/10.3390/BUILDINGS12030360>
- Hao, L., Xiao, J., Sun, J., Xia, B., & Cao, W. (2022). Thermal conductivity of 3D printed concrete with recycled fine aggregate composite phase change materials. *Journal of Cleaner Production*, 364, 132598. <https://doi.org/10.1016/J.JCLEPRO.2022.132598>
- Jaji, M. B., van Zijl, G. P. A. G., & Babafemi, A. J. (2024). Durability and pore structure of metakaolin-based 3D printed geopolymer concrete. *Construction and Building Materials*, 422, 135847. <https://doi.org/10.1016/J.CONBUILDMAT.2024.135847>
- Jiang, Q., Liu, Q., Wu, S., Zheng, H., & Sun, W. (2022). Modification effect of nanosilica and polypropylene fiber for extrusion-based 3D printing concrete: Printability and mechanical anisotropy. *Additive Manufacturing*, 56, 102944. <https://doi.org/10.1016/J.ADDMA.2022.102944>
- Li, P. P., Brouwers, H. J. H., Chen, W., & Yu, Q. (2020). Optimization and characterization of high-volume limestone powder in sustainable ultra-high performance concrete. *Construction and Building Materials*, 242, 118112. <https://doi.org/10.1016/J.CONBUILDMAT.2020.118112>

- Liu, C., Wang, Z., Wu, Y., Liu, H., Zhang, T., Wang, X., & Zhang, W. (2023a). 3D printing concrete with recycled sand: The influence mechanism of extruded pore defects on constitutive relationship. *Journal of Building Engineering*, 68, 106169. <https://doi.org/10.1016/J.JOBE.2023.106169>
- Liu, C., Zhang, Y., & Bantia, N. (2023b). Unveiling pore formation and its influence on micromechanical property and stress distribution of 3D printed foam concrete modified with hydroxypropyl methylcellulose and silica fume. *Additive Manufacturing*, 71, 103606. <https://doi.org/10.1016/J.ADDMA.2023.103606>
- Liu, H., Liu, C., Bai, G., Wu, Y., He, C., Zhang, R., & Wang, Y. (2022a). Influence of pore defects on the hardened properties of 3D printed concrete with coarse aggregate. *Additive Manufacturing*, 55, 102843. <https://doi.org/10.1016/J.ADDMA.2022.102843>
- Liu, H., Liu, C., Wu, Y., Bai, G., He, C., Zhang, R., & Wang, Y. (2022b). Hardened properties of 3D printed concrete with recycled coarse aggregate. *Cement and Concrete Research*, 159, 106868. <https://doi.org/10.1016/J.CEMCONRES.2022.106868>
- Liu, J., Setunge, S., & Tran, P. (2022). 3D concrete printing with cement-coated recycled crumb rubber: Compressive and microstructural properties. *Construction and Building Materials*, 347, 128507. <https://doi.org/10.1016/J.CONBUILDMAT.2022.128507>
- Liu, J., Tran, P., Nguyen Van, V., Gunasekara, C., & Setunge, S. (2023). 3D printing of cementitious mortar with milled recycled carbon fibres: Influences of filament offset on mechanical properties. *Cement and Concrete Composites*, 142, 105169. <https://doi.org/10.1016/J.CEMCONCOMP.2023.105169>
- Liu, Q., Jiang, Q., Huang, M., Xin, J., & Chen, P. (2022). The fresh and hardened properties of 3D printing cement-base materials with self-cleaning nano-TiO₂: An exploratory study. *Journal of Cleaner Production*, 379, 134804. <https://doi.org/10.1016/J.JCLEPRO.2022.134804>
- Ma, L., Zhang, Q., Lombois-Burger, H., Jia, Z., Zhang, Z., Niu, G., & Zhang, Y. (2022). Pore structure, internal relative humidity, and fiber orientation of 3D printed concrete with polypropylene fiber and their relation with shrinkage. *Journal of Building Engineering*, 61, 105250. <https://doi.org/10.1016/J.JOBE.2022.105250>
- Markin, V., Krause, M., Otto, J., Schröfl, C., & Mechtcherine, V. (2021). 3D-printing with foam concrete: From material design and testing to application and sustainability. *Journal of Building Engineering*, 43, 102870. <https://doi.org/10.1016/J.JOBE.2021.102870>
- Motalebi, A., Khondoker, M. A. H., & Kabir, G. (2024). A systematic review of life cycle assessments of 3D concrete printing. *Sustainable Operations and Computers*, 5, 41–50. <https://doi.org/10.1016/J.SUSOC.2023.08.003>
- Nedunuri, S. S. S. A., Sertse, S. G., & Muhammad, S. (2020). Microstructural study of Portland cement partially replaced with fly ash, ground granulated blast furnace slag, and silica fume as determined by pozzolanic activity. *Construction and Building Materials*, 238, 117561. <https://doi.org/10.1016/J.CONBUILDMAT.2019.117561>
- Nodehi, M., Aguayo, F., Nodehi, S. E., Gholampour, A., Ozbakkaloglu, T., & Gencel, O. (2022). Durability properties of 3D printed concrete (3DPC). *Automation in Construction*, 142, 104479. <https://doi.org/10.1016/J.AUTCON.2022.104479>
- Özalp, F., & Dilşad Yılmaz, H. (2020). Fresh and Hardened Properties of 3D High-Strength Printing Concrete and Its Recent Applications. *Transactions of Civil Engineering*, 1, 319–330. <https://doi.org/10.1007/s40996-020-00370-4>
- Pasupathy, K., Ramakrishnan, S., & Sanjayan, J. (2022). Enhancing the properties of foam concrete 3D printing using porous aggregates. *Cement and Concrete Composites*, 133, 104687. <https://doi.org/10.1016/J.CEMCONCOMP.2022.104687>
- Pham, L., Tran, P., & Sanjayan, J. (2020). Steel fibres reinforced 3D printed concrete: Influence of fibre sizes on mechanical performance. *Construction and Building Materials*, 250, 118785. <https://doi.org/10.1016/J.CONBUILDMAT.2020.118785>
- Rutzen, M., Schulz, M., Moosburger-Will, J., Lauff, P., Fischer, O., & Volkmer, D. (2021). 3D printing is an automated manufacturing method for a carbon fiber-reinforced cementitious composite with outstanding flexural strength (105 N/mm²). *Materials and Structures/Materiaux et Constructions*, 54(6), 1–20. <https://doi.org/10.1617/S11527-021-01827-2>
- Safiuddin, M., & Hearn, N. (2005). Comparison of ASTM saturation techniques for measuring the permeable porosity of concrete. *Cement and Concrete Research*, 35(5), 1008–1013. <https://doi.org/10.1016/J.CEMCONRES.2004.09.017>
- Singh, A., Liu, Q., Xiao, J., & Lyu, Q. (2022). Mechanical and macrostructural properties of 3D printed concrete dosed with steel fibers under different loading directions. *Construction and Building Materials*, 323, 126616. <https://doi.org/10.1016/J.CONBUILDMAT.2022.126616>
- Skibicki, S., Pułtorak, M., Kaszyńska, M., Hoffmann, M., Ekiert, E., & Sibera, D. (2022). The effect of using recycled PET aggregates on the mechanical and durability properties of 3D printed mortar. *Construction and Building Materials*, 335, 127443. <https://doi.org/10.1016/J.CONBUILDMAT.2022.127443>
- Slavcheva, G. S. (2019). Drying and shrinkage of cement paste for 3D printable concrete. *IOP Conference Series: Materials Science and Engineering*, 481(1), 012043. <https://doi.org/10.1088/1757-899X/481/1/012043>
- Tan, C. T., Yew, M. K., Yew, M. C., Lee, F. W., Lim, S. K., Beh, J. H., Lee, J. C., & Lim, J. H. (2025). Mechanical property enhancement in concrete composites with hybrid polypropylene fibre reinforcement. *Scientific Reports*, 15(1), 24986. <https://doi.org/10.1038/S41598-025-04219-6>
- Van der Putten, J., De Volder, M., Van den Heede, P., Deprez, M., Cnudde, V., De Schutter, G., & Van Tittelboom, K. (2022). Transport properties of 3D printed cementitious materials with a prolonged time gap between successive layers. *Cement and Concrete Research*, 155, 106777. <https://doi.org/10.1016/J.CEMCONRES.2022.106777>
- Vergara, L. A., & Colorado, H. A. (2020). Additive manufacturing of Portland cement pastes with additions of kaolin, superplasticizer and calcium carbonate. *Construction and Building Materials*, 248, 118669. <https://doi.org/10.1016/J.CONBUILDMAT.2020.118669>
- Vishruthi, M., Raghavendra, S., Ravi Teja, Y., & Anand, K. B. (2021). Evaluation of Cementitious Mixes for Printing. *Lecture Notes in Civil Engineering*, 97, 611–623. https://doi.org/10.1007/978-3-030-55115-5_56
- Wang, D., Xiao, J., Sun, B., Zhang, S., & Poon, C. S. (2023). Mechanical properties of 3D printed mortar cured by CO₂. *Cement and Concrete Composites*, 139, 105009. <https://doi.org/10.1016/J.CEMCONCOMP.2023.105009>
- Wang, L., Ma, H., Li, Z., Ma, G., & Guan, J. (2021). Cementitious composites blending with high belite sulfoaluminate and medium-heat Portland cements for large-scale 3D printing. *Additive Manufacturing*, 46, 102189. <https://doi.org/10.1016/J.ADDMA.2021.102189>

- Wang, L., Xiao, W., Wang, Q., Jiang, H., & Ma, G. (2022). Freeze-thaw resistance of 3D-printed composites with desert sand. *Cement and Concrete Composites*, 133, 104693. <https://doi.org/10.1016/J.CEMCONCOMP.2022.104693>
- Wang, X., Jia, L., Jia, Z., Zhang, C., Chen, Y., Ma, L., Wang, Z., Deng, Z., Banthia, N., & Zhang, Y. (2022). Optimization of 3D printing concrete with coarse aggregate via proper mix design and printing process. *Journal of Building Engineering*, 56, 104745. <https://doi.org/10.1016/J.JOBE.2022.104745>
- Worrell, E., Price, L., Martin, N., Hendriks, C., & Meida, L. O. (2001). Carbon dioxide emissions from the global cement industry. *Annual Review of Energy and the Environment*, 26(Volume 26, 2001), 303–329. <https://doi.org/10.1146/ANNUREV.ENERGY.26.1.303/CITE/REFWORKS>
- Yang, Y., Wu, C., Liu, Z., Wang, H., & Ren, Q. (2022). Mechanical anisotropy of ultra-high performance fibre-reinforced concrete for 3D printing. *Cement and Concrete Composites*, 125, 104310. <https://doi.org/10.1016/J.CEMCONCOMP.2021.104310>
- Yao, H., Xie, Z., Li, Z., Huang, C., Yuan, Q., & Zheng, X. (2022). The relationship between the rheological behavior and interlayer bonding properties of 3D printing cementitious materials with the addition of attapulgite. *Construction and Building Materials*, 316, 125809. <https://doi.org/10.1016/J.CONBUILDMAT.2021.125809>
- Yuan, Q., Xie, Z., Yao, H., Huang, T., Li, Z., & Zheng, X. (2022). Effect of polyacrylamide on the workability and interlayer interface properties of 3D printed cementitious materials. *Journal of Materials Research and Technology*, 19, 3394–3405. <https://doi.org/10.1016/J.JMRT.2022.06.093>
- Zeng, Q., Chen, S., Yang, P., Peng, Y., Wang, J., Zhou, C., Wang, Z., & Yan, D. (2020). Reassessment of mercury intrusion porosimetry for characterizing the pore structure of cement-based porous materials by monitoring the mercury entrapments with X-ray computed tomography. *Cement and Concrete Composites*, 113, 103726. <https://doi.org/10.1016/J.CEMCONCOMP.2020.103726>
- Zhang, Y., Yunsheng, Z., Lin, Y., Guojian, L., Yidong, C., Shiwei, Y., Du, H., Zhang, Y., Chen, Y., Chen, Á. Y., Yang, L., Liu, G., Yu, S., & Du, H. (2021). Hardened properties and durability of large-scale 3D printed cement-based materials. *Materials and Structures*, 54(1), 45. <https://doi.org/10.1617/s11527-021-01632-x>
- Zhao, Y., Gao, Y., Chen, G., Li, S., Singh, A., Luo, X., Liu, C., Gao, J., & Du, H. (2023). Development of low-carbon materials from GGBS and clay brick powder for 3D concrete printing. *Construction and Building Materials*, 383, 131232. <https://doi.org/10.1016/J.CONBUILDMAT.2023.131232>